

A PC-Based Logic Simulator Using a Look-Up Table Cascade Emulator

Hiroki NAKAHARA^{†a)}, Student Member, Tsutomu SASAO^{†b)}, and Munehiro MATSUURA^{†c)}, Members

SUMMARY This paper represents a cycle-based logic simulation method using an LUT cascade emulator, where an LUT cascade consists of multiple-output LUTs (cells) connected in series. The LUT cascade emulator is an architecture that emulates LUT cascades. It has a control part, a memory for logic, and registers. It connects the memory to registers through a programmable interconnection circuit, and evaluates the given circuit stored in the memory. The LUT cascade emulator runs on an ordinary PC. This paper also compares the method with a Levelized Compiled Code (LCC) simulator and a simulator using a Quasi-Reduced Multi-valued Decision Diagram (QRMD). Our simulator is 3.5 to 10.6 times faster than the LCC, and 1.1 to 3.9 times faster than the one using a QRMD. The simulation setup time is 2.0 to 9.8 times shorter than the LCC. The necessary amount of memory is 1/1.8 to 1/5.5 of the one using a QRMD.

key words: LUT cascade, bdd-for-cf, functional decomposition

1. Introduction

With the increase of the integration of LSIs, the time for the verification of the design increases. Thus, high-speed logic simulators are needed.

Logic simulators can be roughly divided into two types: event-driven simulators and cycle-based simulators. In an event-driven simulator, only the outputs of the gates whose input signals change are evaluated. On the other hand, in a cycle-based logic simulator, the operation order of gates are determined statically beforehand, and all the outputs of the gates are evaluated for each clock cycle. Although the cycle-based logic simulator does not perform the timing verification, it is often faster than the event-driven simulator.

An LCC [1] is a kind of a cycle-based logic simulator using a general-purpose CPU. An LCC generates a program code for each gate of a logic circuit, and evaluates the circuit in a topological order from the inputs towards the outputs. In this paper, we will present a cycle-based logic simulator using an LUT cascade emulator. An LUT cascade emulator [2] consists of a control part, memories, and registers. Each register is connected to a programmable interconnection circuit, and the LUT cascade emulator evaluates the logic circuit stored in the memory. Murgai-Hirose-Fujita

[10] also developed a logic simulator using large memories. Their method first converts a given circuit into a random logic network of single-output LUTs, then stores them in the memory, and finally evaluates the circuit by an event-driven logic simulator implemented by a hardware accelerator. In our method, we first convert the given circuit into a cascade rather than random logic, so the control part is simpler than Murgai-Hirose-Fujita's method. Also, our method uses multiple-output LUTs rather than single-output LUTs. In this paper, we consider a software-based logic simulation system where the LUT cascade emulator is simulated on a PC. Compared with the hardware-based logic emulator, a logic simulator using a standard PC is much cheaper, and can be enhanced with the improvement of the performance of PCs. Our simulator outperforms commercial logic simulators [13].

This paper is an extended version of [13].

2. LUT Cascade Emulator

Figure 1 shows a model of a sequential circuit, where X denotes inputs, Z denotes outputs, Y denotes the inputs to flip-flops, Y' denotes the outputs of flip-flops, and $|Y|$ denotes the number of state variables. We first introduce an **LUT cascade** [3] that realizes the combinational part of a sequential circuit, then introduce the LUT cascade emulator that emulates the LUT cascade.

2.1 LUT Cascade

An LUT cascade is shown in Fig. 2, where multiple-output LUTs (**cells**) are connected in series to realize a multiple-output function. The wires connecting adjacent cells are called **rails**. Also, each cells may have external outputs in addition to the rail outputs. In this paper, X_i denotes the **external inputs** to the i -th cell; Y'_i denotes the **state inputs** to the i -th cell; Z_i denotes the **external outputs** of the i -th cell;

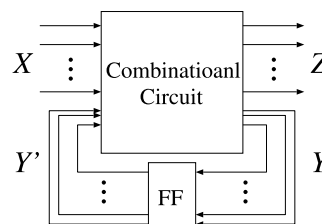


Fig. 1 A model for a sequential circuit.

Manuscript received March 8, 2006.

Final manuscript received June 12, 2006.

[†]The authors are with the Department of Computer Science and Electronics, Kyushu Institute of Technology, Iizuka-shi, 820-8502 Japan.

a) E-mail: nakahara@aries01.cse.kyutech.ac.jp

b) E-mail: sasao@cse.kyutech.ac.jp

c) E-mail: matsuura@cse.kyutech.ac.jp

DOI: 10.1093/ietfec/e89-a.12.3471

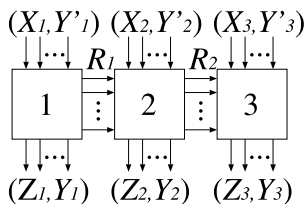


Fig. 2 LUT cascade.

Y_i denotes the **state outputs** of the i -th cell; R_{i-1} denotes the **rail inputs** to the i -th cell; and R_i denotes the **rail outputs** from the i -th cell. We can obtain an LUT cascade by applying **functional decompositions** repeatedly to the BDD that represents the multiple-output function [4].

Definition 2.1: Let $\vec{X} = (x_1, x_2, \dots, x_n)$ be the input variables, $\vec{Y} = (y_1, y_2, \dots, y_m)$ be the output variables, and $\vec{f} = (f_1(\vec{X}), f_2(\vec{X}), \dots, f_m(\vec{X}))$ be the corresponding output functions. **The characteristic function of the multiple-output function** is $\vec{\chi}(\vec{X}, \vec{Y}) = \bigwedge_{i=1}^m (y_i \equiv f_i(\vec{X}))$.

The characteristic function of an n -input m -output function is a two-valued logic function with $(n + m)$ inputs. It has input variables x_i ($i = 1, 2, \dots, n$), and output variables y_j for output f_j . Let $B = \{0, 1\}$, $\vec{a} \in B^n$, $\vec{F} = (f_1(\vec{a}), f_2(\vec{a}), \dots, f_m(\vec{a})) \in B^m$, and $\vec{b} \in B^m$. Then, the characteristic function satisfies the relation:

$$\vec{\chi}(\vec{a}, \vec{b}) = \begin{cases} 1 & (\text{when } \vec{b} = \vec{F}(\vec{a})) \\ 0 & (\text{otherwise}) \end{cases}$$

Definition 2.2: A **support variable** of a function f is a variable on which f actually depends.

Definition 2.3: [5] **The BDD_for_CF** of a multiple-output function $\vec{f} = (f_1, f_2, \dots, f_m)$ is the ROBDD [9] for the characteristic function $\vec{\chi}$. In this case, we assume that the root node is in the top of the BDD, and the variable y_i is below the support variable of f_i , where y_i is the variable representing f_i .

Definition 2.4: **The width of the BDD_for_CF** at height k is the number of edges crossing the section of the graph between x_k and x_{k+1} , where the edges incident to the same nodes are counted as one. Also, in counting the width of the BDD_for_CF, we ignore the edges that incident to the constant 0 node.

Let X_1 and X_2 be sets of input variables, Y_1 and Y_2 be sets of output variables, (X_1, Y_1, X_2, Y_2) be the variable ordering of a BDD_for_CF for the multiple-output function $\vec{f} = (f_1, f_2, \dots, f_m)$, and W be the width of the BDD_for_CF at the height (X_1, Y_1) in Fig. 3. By applying functional decomposition to \vec{f} , we obtain the network in Fig. 4, where the number of lines connecting two blocks is $t = \lceil \log_2 W \rceil$ [4].

Theorem 2.1: [5] Let μ_{max} be the maximum width of the BDD_for_CF that represents an n -input logic function \vec{f} . If

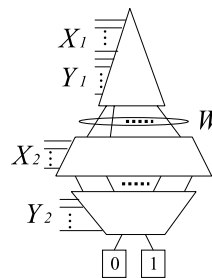


Fig. 3 BDD_for_CF.

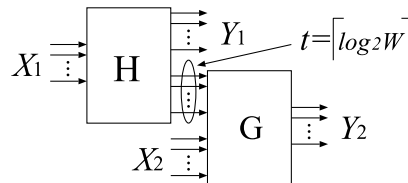


Fig. 4 Functional decomposition.

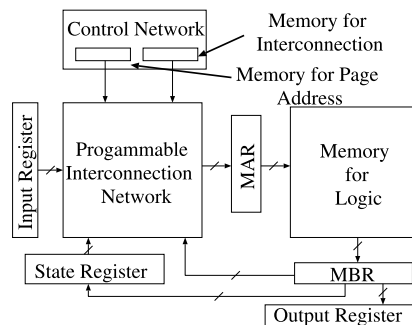


Fig. 5 LUT cascade emulator.

$u = \lceil \log_2 \mu_{max} \rceil \leq k - 1$, then \vec{f} can be realized by a circuit shown in Fig. 4, where $|X_1| = k$. By applying functional decompositions $s - 1$ times, we have the cascade having the structure of Fig. 2.

2.2 LUT Cascade Emulator

Figure 5 shows an **LUT cascade emulator** for a sequential circuit.

An LUT cascade emulator stores the cell data of an LUT cascade in the **Memory for Logic**. The address of cell data is calculated from inputs, state variables, and rail outputs of the preceding cell. The LUT cascade emulator reads the cell outputs from the memory for logic, and send them to the **State Register** and the **Output Register**. The **Input Register** stores the values of the primary inputs; the **MAR** (Memory Address Register) stores the address of the memory; the **MBR** (Memory Buffer Register) stores the outputs of the memory; the **Programmable Interconnection Network** connects the input register, the state register, and the MBR to the MAR; the **Memory for Interconnection** stores data for the interconnections; **Memory for Page Address** stores data for the page address; and the **Control Net-**

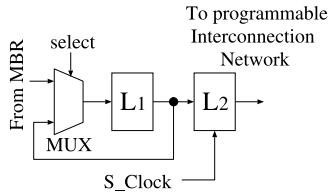


Fig. 6 Double rank flip-flop.

work generates necessary signals to obtain functional values.

To emulate a sequential circuit, the LUT cascade emulator stores state variables and output variables in the registers. Figure 6 shows the **Double-Rank Flip-Flop** for the state register and the output register, where L_1 and L_2 are D-latches. Set the select signals to high when all the cells in a cascade are evaluated, and send the values into L_1 latches. When all the cascades are evaluated, the values of the state variables are sent to L_2 latches. This can be done by adding a pulse to S_Clock.

3. Synthesis of the LUT Cascade Emulator

The data for a BDD_for_CF can be too large to be stored in a memory of the computer. Even if the BDD_for_CF is stored in a memory of the computer, it can be too large to be realized by an LUT cascade. Also, constructing a single BDD_for_CF for all the outputs is inefficient, since the optimization of a large BDD_for_CF is time consuming. In this paper, we first partition the given circuit into groups, and then construct a BDD_for_CF for each group.

Previous approach [13] partitions the output functions into groups so that the total number of cells is minimized. The method [13] uses a simple heuristic method to partition the outputs quickly. However, when the BDD_for_CF representing a single output function is excessively large, this method fails.

In this paper, we partition the circuit rather than the outputs. Although we have to introduce connection signals between groups, we can represent the circuits that are too large for the previous method [13].

3.1 Graph Representation of a Circuit

To partition the circuit, we represent the given circuit by a directed-graph. We replace logic modules with nodes, and interconnections with edges. Also, we divide feedback lines into feedback inputs and feedback outputs, and replace them with edges.

Definition 3.5: A **primary input node** denotes a primary input or a feedback input. A **primary output node** denotes a primary output or a feedback output. A **logic module node** denotes a logic module.

Example 3.1: Figure 8 illustrates a graph representing the circuit in Fig. 7. In Fig. 8, $x_0, x_1, x_2, x_3,$ and z'_1 are primary input nodes, and z_0 and z_1 are primary output nodes.

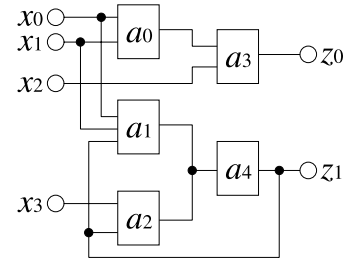


Fig. 7 A example for a circuit.

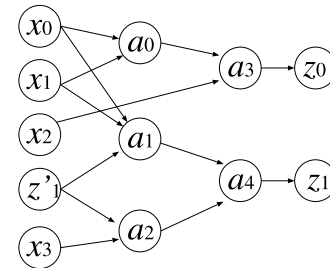


Fig. 8 A graph representing Fig. 7.

$a_0, a_1, a_2, a_3,$ and a_4 are logic module nodes.

Definition 3.6: Let A be a set of logic module nodes. The **input nodes for A** are the nodes that have incident edges to A , denoted by $In(A)$. Similarly, the **output nodes for A** are the nodes that have incident edges from A , denoted by $Out(A)$.

3.2 Partition of a Circuit

We formulate the partition problem for the given circuit as follows:

Problem 3.1: Suppose that the given circuit is represent by a graph. Let A be the set of the logic module nodes in the graph. Then, partition the set A into subsets A_j ($j = 1, 2, \dots, g$) as follows:

1. $A_i \cap A_j = \phi$ ($i \neq j$), $\bigcup_{j=1}^g A_j = A$.
2. A_j can be realized by an LUT cascade.
3. $Node(A_j) \leq ThNode$, where $ThNode$ denotes the maximum number of nodes for a group, and $Node(A_j)$ denotes the number of nodes in the BDD_for_CF that represents A_j .

Although several partitioning algorithms (e.g. by liner programming, or by dynamic programming) have been reported [18]–[20], they require long computation time. In this paper, we trade the partition time and the quality of the partitioned circuits.

Algorithm 3.1: (Partition the Circuit into Groups and Construct BDD_for_CFs) Let A be the set of the logic module nodes that represent the given circuit, g be the number of block in the partition, X be the set of the primary input

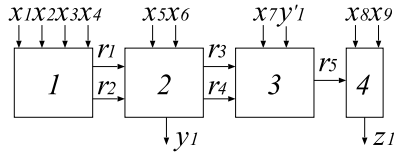


Fig. 9 Example of LUT cascade.

nodes, A_g be the set of nodes under selection, B be the set of nodes after selection, C be the set of candidate nodes, and $ThNode$ be the maximum number of nodes for each BDD_for_CF.

- 1: $B \leftarrow X, C \leftarrow Out(X), g \leftarrow 0, A_0 \leftarrow \phi$.
- 2: **while**($C \neq \phi$) {
- 3: Select $a_j \in C$ such that $|In(A_g \cup a_j)| + |Out(A_g \cup a_j)|$ is minimum.
- 4: Construct the BDD_for_CF that represents $A_g \cup a_j$.
- 5: **if**($Node(A_g \cup a_j) \leq ThNode$ && ($A_g \cup a_j$ can be realized by a cascade)) {
- 6: $A_g \leftarrow A_g \cup a_j, C \leftarrow C \cup Out(a_j) - a_j$.
- 7: } **else** {
- 8: $B \leftarrow B \cup \{A_g\}$.
- 9: $g \leftarrow g + 1$.
- 10: $A_g \leftarrow a_j, C \leftarrow Out(a_j)$.
- 11: } }
- 12: }
- 13: Terminate.

Algorithm 3.1 finds a logic module node that minimizes the total number of inputs and outputs nodes (line 3). Then, it constructs the BDD_for_CF, and checks whether the number of nodes in BDD_for_CF is less than the $ThNode$ or not (line 5). Also, it checks whether the group can be realized by a cascade or not (line 5). Algorithm 3.1 partitions the given circuit quickly, since it searches for the nodes of the circuit only once.

3.3 Memory Packing

By Algorithm 3.1, we represent a given multiple-output function by a set of BDD_for_CFs. Then, we construct the LUT cascades for them, and then store the LUT data into the memory of the LUT cascade emulator.

Example 3.2: Figure 9 shows an LUT cascade consisting of 4-input cells. Figure 10(a) illustrates the memory map of cell data, where the memory for logic has 6-bit address inputs, and each word consists of four bits. The dark areas in the figure are unused, and P_i denotes the page number. (End of Example)

In Example 3.2, each cell data is stored in a separate page of the memory. The data of a cell must be stored in the same page, and must be read simultaneously. If there are any extra space in the same page, then multiple cell data can be stored in the same page. This method to reduce the memory area is **memory-packing** [6].

Example 3.3: In Fig. 10(a), by storing the cell data r_5 and z_1 to Page 1, we have the memory map in Fig. 10(b), where a half of the memory is enough to store all the

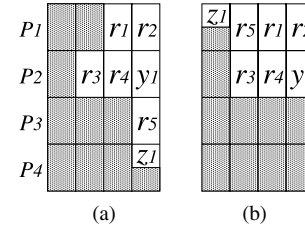


Fig. 10 Example of memory-packing.

data.

(End of Example)

4. Logic Simulation on an LUT Cascade Emulator

4.1 Generation of the Execution Code for Simulation

Figure 11 shows the logic simulation system using an LUT cascade emulator. First, it partitions the Verilog-VHDL netlist-code describing the given circuit, and constructs BDD_for_CFs by Algorithm 3.1. Then, it reduces the number of nodes of BDDs by optimizing variable orders [7]. Next, it generates LUT cascades from BDDs using functional decompositions described in Chapter 2, and it maps them into the memory of the LUT cascade emulator. Also, it generates the C code that describes the control circuit of the LUT cascade emulator. Next, it compiles the C code into the execution code for simulation of the LUT cascade emulator. And, finally the simulator on a PC evaluates the outputs of the given circuit by using the memory of the LUT cascade emulator.

4.2 Program Code for the LUT Cascade Emulator

This system generates the program code that describes the following operations:

- Step 1 Set the input register, and initialize the state register.
 - Set the input values to the input register. Also, initialize to values of the state register.
- Step 2 Evaluate each cell.
 - Step 2.1 Simulate the programmable interconnection network.
 - Generate the address of the memory for logic from the values of the input register, the state register, the MBR, and the page address.
 - Step 2.2 Read the memory for logic.
 - Read the content of the memory for logic using the address generated in Step 2.1.
 - Step 2.3 Distribute the output values of the memory for logic.
 - Send the values read in Step 2.2 to the output register and to the state register.
- Step 3 Perform the state transition.
 - Update the output values of the state register by using S_Clock.
 - Sending each memory output to each register usually

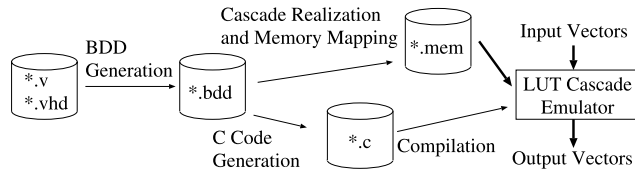


Fig. 11 The logic simulation system using LUT cascade emulator.

consumes CPU time. Fortunately, the memory outputs are stored in the order of primary outputs, state outputs, and rail outputs. For a 32-bit processor, we can evaluate up to 32 outputs at a time. To obtain required outputs, we shift the memory outputs covered by a mask, and assign into a 32-bit variable. In this way, we can evaluate the multiple output simultaneously. Also, there is an additional merit for performing the state transition. Let $|Y|$ be the number of state variables of the given logic function, then the necessary number of evaluations for the state transition is $\left\lceil \frac{|Y|}{32} \right\rceil$ for a 32-bit machine.

Since cascades have many fewer signal lines than the original circuit, the compilation time for cascades are much shorter than that of the conventional LCC method.

4.3 Analysis of Simulation Time

When an LUT cascade emulator is implemented on a dedicated hardware [2], the evaluation time is proportional to the number of cells. However, when an LUT cascade emulator is implemented on a standard PC, we need extra time, since the inputs and outputs of a cell must be evaluated sequentially.

To do high-speed simulation for an LUT cascade emulator on a PC, we consider two objects:

- a. Reduction of the number of cells.
This can be done by increasing the number of inputs of each cell. However, the increase of the number of inputs of each cell also increases the evaluation time per cell, which will be explained later.
- b. Reduction of the number of cell inputs.
This decreases the evaluation time per cells, but increases the number of cells.

To find the best strategy, we did the following experiments. We implemented 10 MCNC benchmark functions [8] on the LUT cascade emulator. By changing the maximum number of inputs for cells, we obtained the average number of cell inputs, the number of cells, and the execution time of the LUT cascade emulator. Figure 12 shows the experimental results, where the horizontal axis denotes the maximum number of cell inputs; 0 denotes the lower bound on the maximum number of inputs of cells, that is $\lceil \log_2 \mu_{max} \rceil + 1$; the vertical axis denotes the ratios of the number of cells, the number of the average cell inputs, and simulation time. We set 1.00 to the ratios when the number of cell inputs is $\lceil \log_2 \mu_{max} \rceil + 1$.

Figure 12 shows that the simulation time increases with

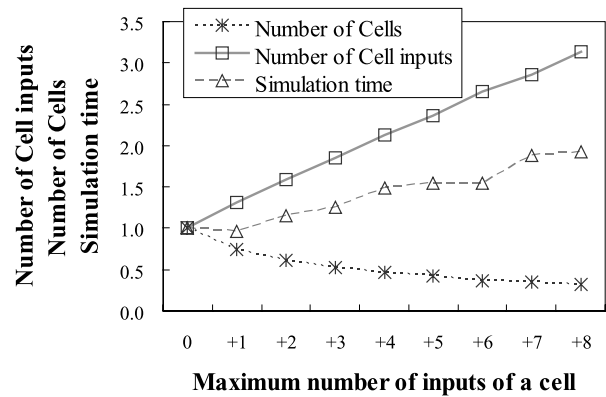


Fig. 12 Relation between the maximum number of cell inputs and simulation time.

the number of cell inputs. The reason for this will be analyzed in Sect. 5.3. Therefore, our strategy is to reduce the number of cell inputs in the LUT cascade emulator.

5. Experimental Results

We implemented Algorithm 3.1 and the simulation system described in Sect. 4.1 in the C programming language. Then, we compared our method with other simulation methods with respect to the simulation time, the simulation setup time, and the size of memories.

5.1 The Benchmark Functions

Table 1 shows the benchmark functions [15], [16] used for simulation. *Name* denotes the name of the benchmark function; *In* denotes the number of primary inputs; *Out* denotes the number of primary outputs; *FF* denotes the number of flip-flops; and *Gate* denotes the number of gates.

5.2 Comparison with LCC

We implemented the LCC simulator in the C programming language. Table 2 compares our method with the LCC. *Name* denotes the name of benchmark function; *Cas* denotes the number of LUT cascades; *Cell* denotes the total number of cells; *ASM* denotes the number of instructions in the assembly code; *Code* denotes the code image size (kilo bytes); *E.in* denotes the average number of external inputs to cells; *P.out* denotes the total number of external output(s); and *S.out* denotes the total number of state output(s). *Sim* denotes the evaluation time (sec). In order to obtain the raw simulation time, we generated one million random test vectors, and obtained the time excluding the setup time for reading and writing vectors. *Setup* denotes the setup time (sec) for the simulation. *Setup* of LCC includes the time for the C-code generation and the compilation, while *Setup* of the LUT cascade emulator includes the time for partition the circuit, BDD generation, LUT cascade synthesis, memory mapping, C-code generation, and the compilation. *Literals* denotes the total number of literals

in expressions of the C-code generated by the LCC. *Ratios* denote that of the simulation setup time and that of the simulation execution time (LCC/LUT cascade emulator). To produce the executable code for LCC, we used gcc compiler with optimization option -O3. Also, we generated program codes for LUT cascade emulator, and compiled them with the same conditions as LCC. In the experiments, we used an IBM PC/AT compatible machine, Pentium4 Xeon 2.8 GHz, L1 Data Cache: 8 KB, L1 Instruction Cache: 12 μ ops, L2 Cache: 512 KB, Memory: 4 GByte, and OS: Redhad (Linux 7.3).

Table 2 shows that the LUT cascade emulator is 3–10 times faster than the LCC. Also, the setup for the LUT cascade emulator is 2–9 times faster than the LCC. Since the size of C-code for *b17*, *b18*, and *b22* were too large, gcc could not optimize the codes with the option. Although we could simulate these benchmarks when we removed the optimize option for gcc, the simulation times were too long. Thus, we excluded these data from Table 2. The code image sizes for the LCC are larger, since the LCC converts all the gates and signals into the C-code. On the other hand, the code image size for the LUT cascade emulator is smaller, since the LUT cascade emulator partition the given circuit into the memory for logic, and only the C-code that emulates the control part is generated. Although the LUT cascade emulator requires extra memory, they can be stored it in the memory of our PC.

To analyze the difference of the simulation time, we compare the estimated values with the experimental values. The number of operations in the LUT cascade emulator is estimated as follows:

$$EST.Cas = E.in \times Cell$$

Table 1 The benchmark functions.

Name	In	Out	FF	Gate	Description
wb_dma	216	215	521	3389	DMA Bridge IP Core
mem_ctrl	115	152	1051	11440	Memory Controller
usb_funct	114	121	1704	12808	USB Function Core
b14	32	54	245	10098	Viper processor (subset)
b15	36	70	449	8922	80386 processor (subset)
b17	37	97	1415	32326	Three copies of b15
b18	36	23	3320	114621	Two copies b14 and Two of b17
b20	32	22	490	20226	A copy of b14 and a modified version of b14
b21	32	22	490	20571	Two copies of b14
b22	32	22	735	29951	A copy of b14 and two modified version of b14

$$+Cell + P.out + S.out + Rail, \quad (1)$$

where, $Rail = Cell - Cas$. The first term of expression (1) denotes the setup time of all the external inputs of the cells; the second term denotes the access time to the memory for logic; the third term denotes the setup time for the output register; the fourth term denotes the setup time for the state register; and the last term denotes the setup time for the rail inputs. In Fig. 13, the right vertical axis denotes the experimental value SIM.Cas (sec), and the left vertical axis denotes the estimated number of operations EST.Cas. Also, we conjecture that *Literals* is proportional to the simulation time for LCC. In Fig. 14, the right vertical axis denotes the experimental value SIM.LCC (sec), and the left vertical axis denotes the estimated number of literals EST.LCC = *Literals*. Figures 13 and 14 show that the SIM.Cas and SIM.LCC can be estimated from EST.Cas and EST.LCC, respectively.

In Figs. 13 and 14, we can see that SIM.Cas is smaller than SIM.LCC, and also EST.Cas (number of operations) is smaller than EST.LCC (number of literals). To analyze these results, we converted the C-codes of the LUT cascade emulator and the LCC into the assembly-instructions. Figure 15 compares the numbers of assembly-instructions and the estimated values. In Fig. 15, the vertical axis denotes the number of instructions. The number of the assembly-instructions for both methods are larger than the numbers of C instructions. Especially, that of the LCC increased. This is because the LCC compiler generates extra codes to evaluate negative literals and logic gates, and to produce the output

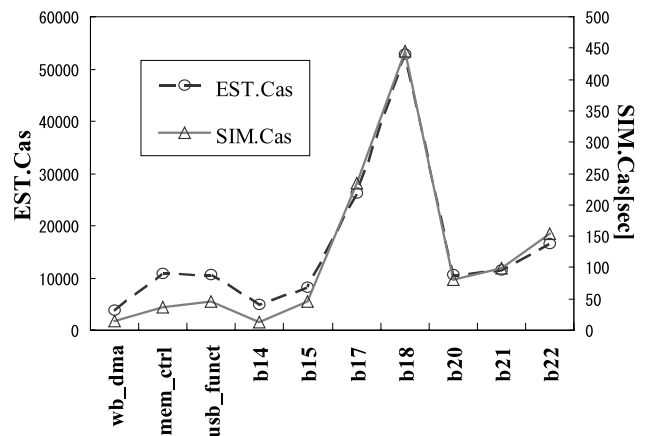


Fig. 13 Simulation time for LUT cascade emulator.

Table 2 Comparison with the LCC.

Name	LUT cascade emulator							LCC					Ratios			
	Cas	Cell	E.in	P.out	S.out	ASM	Code [kbyte]	Setup [sec]	Sim [sec]	Literals	ASM	Code [kbyte]	Setup [sec]	Sim [sec]	Setup	Sim
wb_dma	12	581	3.2	215	521	12876	80	22.2	14.3	13114	35005	173	45.9	61.3	2.0	4.2
mem_ctrl	109	1745	3.5	152	1051	38560	208	136.6	35.9	41189	105076	489	429.0	234.9	3.1	6.5
usb_funct	47	1429	4.1	121	1704	37635	213	138.8	44.9	79667	151404	554	744.9	267.8	5.3	5.9
b14	41	1081	2.8	54	245	17895	98	32.3	12.0	51355	76045	374	250.6	131.5	7.7	10.9
b15	49	1379	3.5	70	449	34288	179	105.7	46.1	67375	104150	432	486.5	165.4	4.6	3.5
b17	121	4147	3.9	97	1415	83993	334	249.4	234.2	—	—	—	—	—	—	—
b18	273	7386	4.7	23	3320	143459	564	1034.1	444.7	—	—	—	—	—	—	—
b20	70	2009	3.0	22	490	36012	183	121.0	80.2	90775	135002	651	982.8	254.4	8.1	3.2
b21	79	2167	3.1	22	490	39033	198	139.9	98.9	106469	174149	859	1372.2	329.3	9.8	3.3
b22	121	2953	3.2	22	735	53002	270	179.0	153.6	—	—	—	—	—	—	—

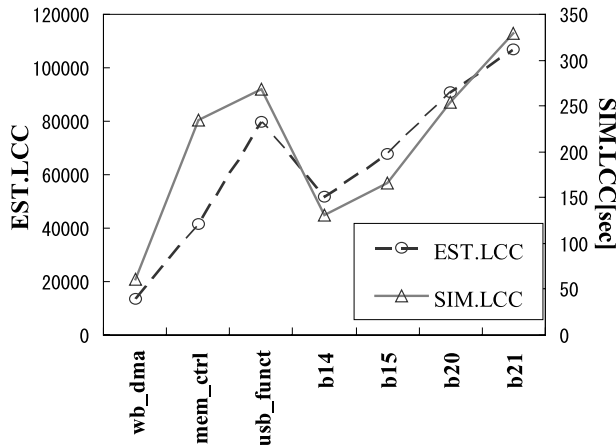


Fig. 14 Simulation time for LCC.

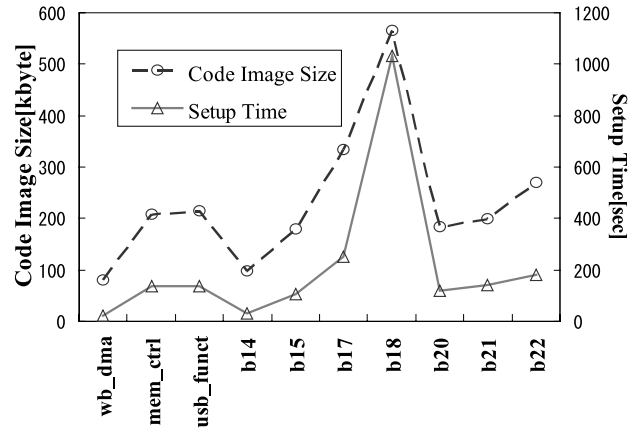


Fig. 16 The code image size for LUT cascade emulator and the simulation setup time.

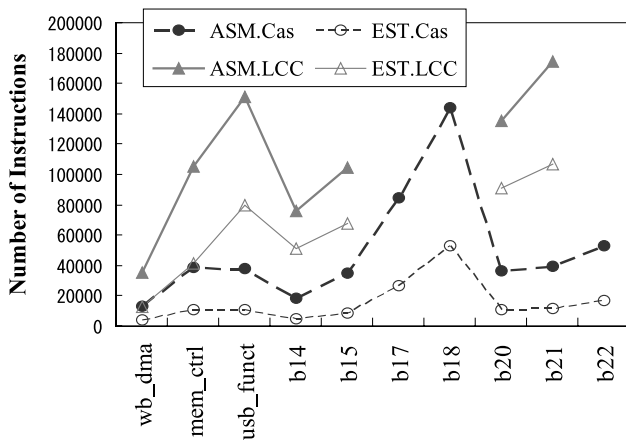


Fig. 15 The assembly-codes and the estimated values.

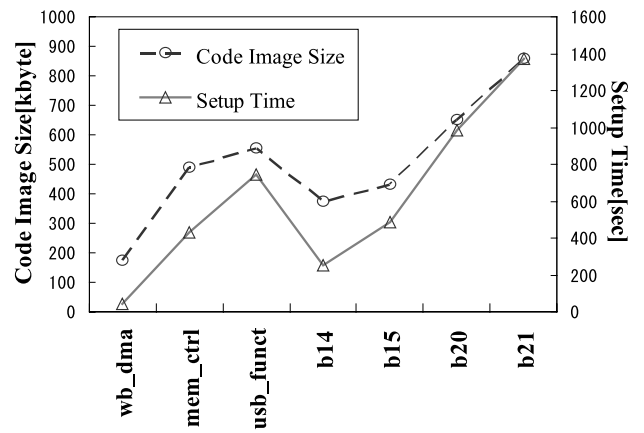


Fig. 17 The code image size for LCC and the simulation setup time.

signals. In the LCC, its operands frequently move between registers and the memory. For the gate with fan-outs, the LCC stores the output values of the gate into a variable temporarily, and uses it as the input of two or more gates. On the other hand, the LUT cascade emulator uses only the rail values stored in a single register variable. Therefore, only the input register, the output register, the memory for logic, and the connections for each group require memory references. Experimental results show that the simulator based on an LUT cascade emulator is 3–10 times faster than the LCC. One reason for this is the difference of the representations: the cascade has many fewer signals than the random logic network. Another reason is the CPU architecture of the PC. The access time of the data in the main memory is about 200 times longer than one in the L1 cache. So, the CPU time heavily depends on the frequency of cache misses. In the case of the LCC simulator, the circuit data and control are mixed, and the instruction data is too large to be stored in the data cache. On the other hand, in the case of an LUT cascade emulator, the cascade data and control data are separated. Control data is in the instruction cache, while the cascade data is in the data cache. Thus, we can expect fewer cache misses in the LUT cascade emulator.

Figures 16 and 17 show the relation between the simulation setup time and the code image size. In these figures, the right vertical axis denotes the simulation setup time (sec), and the left vertical axis denotes the code image size (kilo bytes). These figures show that the code image sizes affects the simulation setup time. The code image size for the LUT cascade emulator is smaller than that of the LCC. Therefore, the LUT cascade emulator is faster than the LCC with respect to the simulation setup time. Note that, in the LUT cascade emulator, we need data for logic in addition to the code.

5.3 Comparison with the QRMD

In this part, we compare with an MDD-based logic simulator. As for the definitions on MDD (Multi-valued Decision Diagram), refer [14], [21]. Let (X_1, X_2, \dots, X_u) be the input variables. When all X_i ($i = 1, 2, \dots, u$) appear in this order in all paths of an MDD (k), the MDD (k) is a QR-MDD (k) (Quasi-Reduced Multi-valued Decision Diagram) with k bits. The length of an arbitrary path in a QR-MDD (k) is equal to u , the number of input variables. Note that, a QR-MDD usually has redundant nodes. By combining the

binary nodes of a BDD into a multi-valued node of 2^k inputs, we obtain a QRMDD (k) [14].

We can generate a code to evaluate the a QRMDD: Store a QRMDD in a table, and use a generic program to evaluate the QRMDD [11]. For example, a table for a QRMDD (2) is obtained from a BDD in Fig. 5.4. Also, Example 5.5 shows the pseudo-code for evaluating a QRMDD (3).

Example 5.4: From a BDD (Fig. 18(a)), by combining the nodes into multi-valued nodes, we have an MDD (Fig. 18(b)). From the MDD (Fig. 18(b)), we have a QRMDD (2) (Fig. 18(c)). From the QRMDD (2) (Fig. 18(c)), we have a table for QRMDD (2) (Fig. 18(d)).

Example 5.5: (Pseudo-code to evaluate QRMDD (3))

1. $ptr \leftarrow root_index; i \leftarrow 0;$
2. $node_input \leftarrow \{x_{i1}, x_{i2}, x_{i3}\};$
3. $ptr \leftarrow table[ptr + node_input];$
4. $i \leftarrow i + 1;$
5. **if** ($i <$ the length of the path for QRMDD (3)) **then** goto 2.
6. Terminate.

The code to evaluate a QRMDD (k) is quite similar to the code to evaluate an LUT cascade emulator. Also, the procedures for pre-computing the circuit beforehand are almost same. The difference between them is a data structure for the function. The QRMDD (k)-based method represents the circuit by multiple QRMDDs (k), and stores them to the table. On the other hand, the LUT cascade emulator represents it by multiple LUT cascades, and stores them to the memory for logic, using memory packing.

Table 3 compares the LUT cascade emulator with the QRMDD (k). *Name*, *Cell*, *Code*, *Setup*, and *Sim* are the

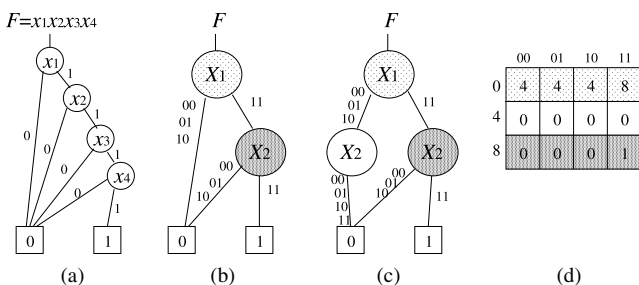


Fig. 18 BDD for $F = x_1x_2x_3x_4$ (a), MDD for F (b), QRMDD(2) for F (c), Table for QRMDD (2) of F (d).

same as Table 2. *Rail* denotes the average number of rails for the LUT cascade emulator; *Mem* denotes the amount of memory (kilo bytes); *Path* denotes the total path length for each QRMDD (k); *Width* denotes the average widths for QRMDDs (k); and *Table* denotes the total memory size of tables (kilo bytes). The environment for the experiment is the same as the case of the LCC. Also for each benchmark, the LUT cascade and the QRMDD (k) are generated from the same BDDs. The setup time for the QRMDD (k) includes the time for partition the circuit, BDD generation, QRMDD (k) generation, table generation, C-code generation, and the compilation. *Ratios* denote that of the simulation setup time, that of the simulation execution time, and that of the memory size (QRMDD (k)/LUT cascade emulator). Since the simulation time for the QRMDD (k) is minimum when $k = 3$, we set to $k = 3$.

Table 3 shows that the LUT cascade emulator is 1.1–3.9 times faster than the QRMDD (3)-based simulator. The setup for the LUT cascade emulator is also faster than that of the QRMDD (3). The memory size for QRMDD (3) is 1.8–5.5 times larger than that of the LUT cascade emulator.

To evaluate the memory size, we compare an estimated memory size with an actual memory size. Let k_i be the number of external inputs of i -th cell, μ_i be the number of rail inputs, and c be the number of cells. Note that, μ_0 denotes the number of rail inputs to the first cell, so $\mu_0 = 0$. Let M_{Cas} be the size of the memory for logic in the LUT cascade emulator. Then, we have

$$M_{Cas} = 2^{k_1 + \mu_0} \mu_1 + 2^{k_2 + \mu_1} \mu_2 + \dots + 2^{k_c + \mu_{c-1}} \mu_c$$

By replacing μ_j ($j = 0, 1, \dots, c$) with $\bar{\mu}$, the average of μ_j , and k_j ($j = 1, 2, \dots, c$) with \bar{k} , the average of k_j , we have the following approximation:

$$\tilde{M}_{Cas} = 2^{\bar{k} + \bar{\mu}} \bar{\mu} c \quad (2)$$

Figure 19 illustrates a node for a QRMDD (k), and Fig. 20 illustrates nodes with respect to X_j . Let p be the path length, w_j ($j = 0, 1, \dots, p$) be the width of the QRMDD (k) with respect to X_j . Note that, w_0 denotes the width on a root node, and $w_0 = 1$. As shown in Fig. 20, one node for a QRMDD (k) can be represented by the table storing 2^k pointers to the next nodes. Let a be the number of bits for the pointer, then the memory size for the table representing a node in a QRMDD (k) is $2^k a$.

Table 3 Comparison with the QRMDD (3).

Name	LUT cascade emulator						QRMDD (3)						Ratios		
	Cell	Rail	Code [kbyte]	Mem [kbyte]	Setup [sec]	Sim [sec]	Path	Width	Code [kbyte]	Table [kbyte]	Setup [sec]	Sim [sec]	Setup	Sim	Mem
wb_dma	581	4.6	80	417	22.2	14.3	622	39.5	92	769	25.8	15.6	1.2	1.1	1.8
mem_ctrl	1745	5.6	208	1838	136.6	35.9	2163	80.8	278	5521	158.4	139.5	1.2	3.9	3.0
usb_funct	1429	4.7	213	1337	138.8	44.9	1970	48.6	248	2297	159.4	105.9	1.1	2.4	2.2
b14	1081	5.4	98	615	32.3	12.0	999	69.0	126	2157	36.8	20.1	1.1	1.7	3.5
b15	1831	5.8	179	975	105.7	46.1	2224	77.2	249	5370	123.8	130.5	1.2	2.8	5.5
b17	4147	4.6	334	2404	249.4	234.2	4930	44.4	428	6845	389.9	565.7	1.3	2.4	2.8
b18	7386	4.8	564	6203	1034.8	444.7	8631	70.3	564	18697	1209.1	999.0	1.2	2.2	3.1
b20	2009	5.2	183	1006	121.0	80.2	2049	57.7	240	3699	131.8	112.7	1.1	2.7	1.4
b21	2167	5.4	198	1253	139.9	98.9	2276	63.1	265	4489	153.4	161.4	1.1	2.8	1.6
b22	2953	5.2	270	1868	179.9	153.6	3223	63.6	366	6415	192.7	326.7	1.1	3.2	2.1

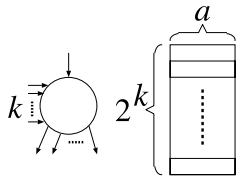


Fig. 19 A table for one node.

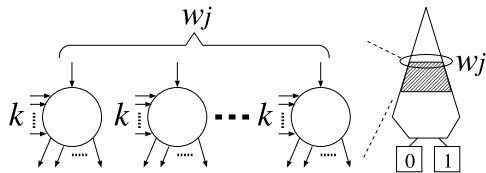
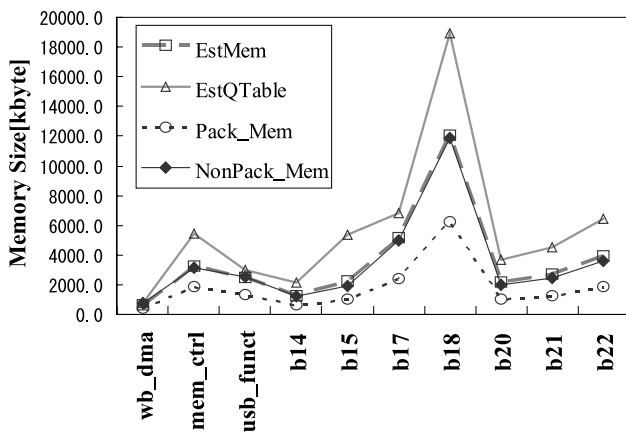

 Fig. 20 A node with respect to X_j .


Fig. 21 Comparison of memory size.

Let $M_{QRMD D}$ be a size of table for a QRMD D (k). Then, we have $M_{QRMD D} = 2^k a \sum_{i=1}^p w_i$. Let \bar{w} be the average of $w_j (j = 0, 1, \dots, p)$. Then, we have following approximation:

$$\tilde{M}_{QRMD D} = 2^k a p \bar{w} \quad (3)$$

When $a = 32$, the experimental results show that $\tilde{M}_{QRMD D}$ is almost the same as actual size of the table. However, \tilde{M}_{Cas} is larger than the actual size of the memory for logic. To investigate this fact, we obtained the size of memory for logic without memory packing. Figure 21 compares $\tilde{M}_{QRMD D}$, \tilde{M}_{Cas} , and the sizes of memory for logic with and without memory packing. The vertical axis denotes the memory size (kilo byte). $NonPack_Mem$ denotes the size of memory for logic without memory packing; $Pack_Mem$ denotes the size of memory for logic with memory packing; $EstMem$ denotes the estimated size \tilde{M}_{Cas} . $EstQTable$ denotes the estimated size $\tilde{M}_{QRMD D}$. Figure 21 shows $Pack$ is 1.9 to 2.1 times smaller than $NonPack_Mem$. Also, $NonPack_Mem$ is almost equal to $EstMem$. Another reason for the difference of the memory sizes is due to the difference of \bar{w} and $\bar{\mu}$. When we generate an LUT cascade, we select functional decomposition that minimizes $\bar{\mu}$ using a dynamic

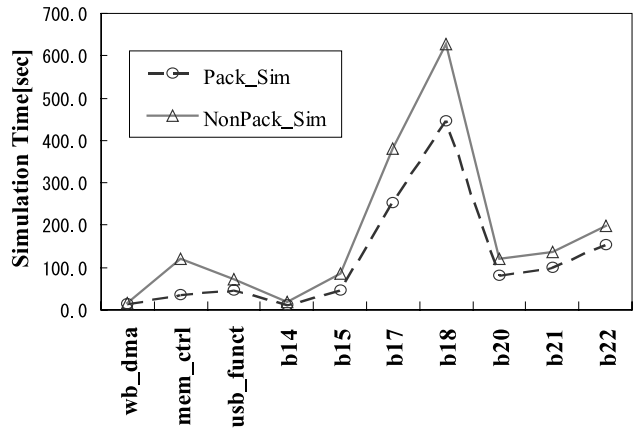


Fig. 22 Influence of memory packing on simulation time.

programming [6], while to construct a QRMD D (3), we do not optimize the size of decompositions. Therefore, $\bar{\mu}$ is smaller than \bar{w} . From Eqs. (2) and (3), these differences affected the memory size.

Both methods perform logic simulation by accessing the data stored in the memory. Thus, the simulation time is affected by the time for accessing memory, the number of memory accesses, and the time for handling the read data. The memory access time heavily depends on the frequency of cache misses. When a cache miss occurs, the CPU accesses the main memory and reads the data. The CPU manages the main memory per page. First, it convert a virtual address into a physical address using a special cache called TLB (Translation Lookaside Buffer), next it accesses the main memory at a high speed and reads the data [17]. Therefore, the size of data stored in a memory affects the memory access time. Figure 22 shows an influence of memory packing on simulation time. In Fig. 22, $Pack_Sim$ denotes the simulation time (sec) with memory packing; $NonPack_Sim$ denotes the simulation time (sec) without memory packing. Since smaller memory tends to have fewer cache misses, $Pack_Sim$ is faster than $NonPack_Sim$. To predict the ratio of simulation time, we define the ratio of simulation time for LUT cascade emulator and QRMD D (k)-based simulator as follows:

$$EST_ratio = \frac{\alpha Path + \beta M_{QRMD D}}{\alpha Cell + \beta M_{Cas}}, \quad (4)$$

where $Path$ denotes the path length, $Cell$ denotes the number of cells, M_{Cas} denotes the size of memory for the LUT cascade emulator, and $M_{QRMD D}$ denotes the size of table for the QRMD D (k). Figure 23 compares SIM_ratio with EST_ratio , where

$$SIM_ratio = \frac{\text{Simulation time for QRMD D (3)-based simulator}}{\text{Simulation time for LUT cascade emulator}} \quad (5)$$

The vertical axis denotes the ratio of the simulation time. In this figure, we set $\alpha = 100$ and $\beta = 1$. Figure 23 shows that EST_ratio has the same tendency as SIM_ratio except for mem_ctrl . In mem_ctrl , many of adjacent cells are stored in the same page of the memory for logic. Since adjacent

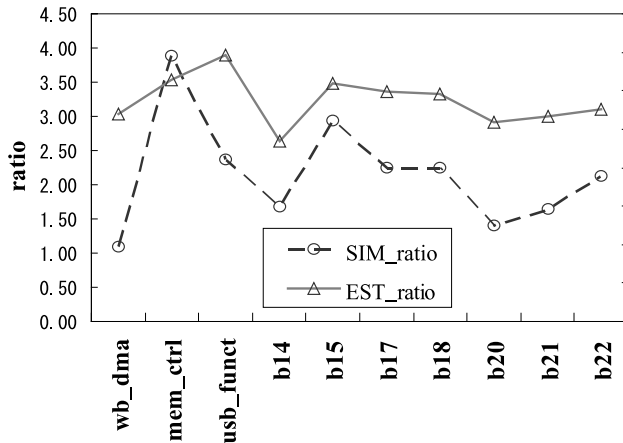


Fig. 23 Estimated value and experimental value.

cells are read continuously, the miss rate of the cache for *mem_ctrl* was low, and the simulation time is short, and *SIM_ratio* is high. We can reduce the simulation time, if we perform memory packing so that adjacent cells are stored in the same page of the memory.

The simulation setup time for both methods are almost same, since the difference of the code image size are also almost the same.

6. Conclusion and Comments

In this paper, we showed a cycle-based logic simulator using the LUT cascade emulator running on a standard PC. This method first converts the circuit into LUT cascades. Then, it stores the LUT data in the memory of the LUT cascade emulator. Next, it generates the program code for the control circuit of the LUT cascade emulator. This paper also compares the method with a LCC simulator and a simulator using a QRMDD. Our simulator is 3.5 to 10.6 times faster than the LCC, and 1.1 to 3.9 times faster than the QRMDD-based one. The simulation setup is 2.0 to 9.8 times faster than the LCC. The amount of memory is 1/1.8 to 1/5.5 of the QRMDD-based simulator. The tricks of our fast simulation are:

1. It replaces many gates into a small number of multi-input multi-output cells. This reduces the number of memory references.
2. It generates the program code that uses both instruction cache and data cache efficiently.
3. It performs memory packing that reduces the cache misses.

The proposed method is a kind of a cycle-based simulator. Note that, special primitives, such as tri-state buffer, are not implemented in the current version.

One of the future projects is to develop a efficient mixed simulator using cycle-based simulation and event-driven simulation.

Acknowledgments

This research is partly supported by Japan Society for the Promotion of Science (JSPS), MEXT, and Kitakyushu Innovative Cluster. Discussions with Prof. Iguchi and Dr. Nagayama were quite useful.

References

- [1] M. Abramovici, M.A. Breuer, and A.D. Friedman, *Digital Systems Testing and Testable Design*, Rev. Print ed., Wiley-IEEE Press, 1994.
- [2] H. Nakahara, T. Sasao, and M. Matsuura, "A design algorithm for sequential circuit using LUT ring," *IEICE Trans. Fundamentals*, vol.E88-A, no.12, pp.3342-3350, Dec. 2005.
- [3] T. Sasao, M. Matsuura, and Y. Iguchi, "A cascade realization of multiple-output function for reconfigurable hardware," *IWLS-2001*, pp.225-300, Lake Tahoe, CA, June 2001.
- [4] T. Sasao and M. Matsuura, "A method to decompose multiple-output logic functions," *Proc. Design Automation Conference*, pp.428-433, San Diego, CA, USA, June 2004.
- [5] P. Ashar and S. Malik, "Fast functional simulation using branching programs," *ICCAD'95*, pp.408-412, Nov. 1995.
- [6] T. Sasao, M. Kusano, and M. Matsuura, "Optimization methods in look-up table rings," *IWLS-2004*, pp.431-437, Temecula, California, USA, June 2004.
- [7] R. Rudell, "Dynamic variable ordering for ordered binary decision diagrams," *ICCAD'93*, pp.42-47, 1993.
- [8] S. Yang, *Logic synthesis and optimization benchmark user guide version 3.0*, MCNC, Jan. 1991.
- [9] R.E. Bryant, "Graph-based algorithms for boolean function manipulation," *IEEE Trans. Comput.*, vol.C-35, no.8, pp.677-691, Aug. 1986.
- [10] R. Murgai, F. Hirose, and M. Fujita, "Logic synthesis for a single large look-up table," *ICCD1995*, pp.415-424, Oct. 1995.
- [11] P.C. McGeer, K.L. McMillan, A. Saldanha, A.L. Sangiovanni-Vincentelli, and P. Scaglia, "Fast discrete function evaluation using decision diagrams," *ICCAD'95*, pp.402-407, Nov. 1995.
- [12] R.K. Brayton, "The future of logic synthesis and verification," in *Logic Synthesis and Verification*, ed. S. Hassoun and T. Sasao, Kluwer Academic Publishers, 2001.
- [13] H. Nakahara, T. Sasao, and M. Matsuura, "A fast logic simulator using an LUT cascade emulator," *ASPDAC 2006*, pp.466-465, Yokohama, Jan. 2006.
- [14] S. Nagayama and T. Sasao, "On the optimization of heterogeneous MDDs," *IEEE Trans. Comput.-Aided Des. Integr. Circuits Syst.*, vol.24, no.11, pp.1645-1659, Nov. 2005.
- [15] S. Davidson, "Characteristics of the ITC'99 benchmark circuits," *ITC'99*, p.1125, Atlantic City, NJ, Sept. 1999.
- [16] opencores.org: <http://www.opencores.org/>
- [17] J.L. Hennessy and D.A. Patterson, *Computer Architecture: A Quantitative Approach*, Morgan Kaufmann Publishers, 1990.
- [18] A.R. Habayeb, "System decomposition, partitioning, and integration for microelectronics," *IEEE Trans. Syst. Sci. Cybern.*, vol.SSC-4, no.2, pp.164-172, July 1968.
- [19] C.H. Haspel, "The automatic packaging of computer circuitry," *1965 IEE International Conv. Rec.*, vol.13, Part 3, pp.4-20, 1965.
- [20] B.W. Kernighan and S. Lin, "An efficient heuristic procedure for partitioning graphs," *Bell Syst. Tech. J.*, vol.49, pp.291-307, 1970.
- [21] T. Kam, T. Villa, R.K. Brayton, and A.L. Sangiovanni Vincentelli, "Multi-valued decision diagrams: Theory and applications," *Multiple-Valued Logic*, vol.4, no.1-2, pp.9-62, 1998.



Hiroki Nakahara was born on September 9, 1980 in Fukuoka Japan, and received B.E. and M.E. degrees from Kyushu Institute of Technology, Iizuka, Japan in 2003 and 2005, respectively. He is now a doctoral student of Kyushu Institute of Technology. His research interest includes logic synthesis, reconfigurable devices, and high-level synthesis.



Tsutomu Sasao received the B.E., M.E., and Ph.D. degrees in electronics engineering from Osaka University, Osaka, Japan, in 1972, 1974, and 1977, respectively. He has held faculty/research positions at Osaka University, Japan, the IBM T.J. Watson Research Center, Yorktown Heights, New York, and the Naval Postgraduate School, Monterey, California. He is now a Professor of the Department of Computer Science and Electronics at the Kyushu Institute of Technology, Iizuka, Japan. His research areas include

logic design and switching theory, representations of logic functions, and multiple-valued logic. He has published more than nine books on logic design, including *Logic Synthesis and Optimization*, *Representation of Discrete Functions*, *Switching Theory for Logic Synthesis*, and *Logic Synthesis and Verification*, Kluwer Academic Publishers, 1993, 1996, 1999, and 2001, respectively. He has served as Program Chairman for the IEEE International Symposium on Multiple-Valued Logic (ISMVL) many times. Also, he was the Symposium Chairman of the 28th ISMVL held in Fukuoka, Japan, in 1998. He received the NIWA Memorial Award in 1979, Distinctive Contribution Awards from the IEEE Computer Society MVL-TC for papers presented at ISMVLs in 1986, 1996, 2003 and 2004, and Takeda Techno-Entrepreneurship Award in 2001. He has served as an Associate Editor of the *IEEE Transactions on Computers*. He is a fellow of the IEEE.



Munehiro Matsuura was born on 1965 in Kitakyushu City, Japan. He studied at the Kyushu Institute of Technology from 1983 to 1989. He received the B.E. degree in Natural Sciences from the University of the Air, in Japan, 2003. He has been working as a Technical Assistant at the Kyushu Institute of Technology since 1991. He has implemented several logic design algorithms under the direction of Professor Tsutomu Sasao. His interests include decision diagrams and exclusive-OR based circuit design.